JOURNAL OF AGRICULTURAL AND FOOD CHEMISTRY

Article

pubs.acs.org/JAFC

Development of Highly Ordered Nanofillers in Zein Nanocomposites for Improved Tensile and Barrier Properties

Boce Zhang and Qin Wang*

Department of Nutrition and Food Science, University of Maryland, 0112 Skinner Building, College Park, Maryland 20742, United States

ABSTRACT: It has been a long-lasting challenge to prepare highly ordered biopolymer nanocomposites to optimize or tune the desired mechanical and barrier properties of the nanocomposite film. In this study, we developed a simple and cost-effective method to synthesize highly ordered zein nanocomposites. The method involved the synthesis of magnetic iron oxide (Fe_3O_4) nanofiller and the preparation of a highly ordered structure by *in situ* nanofiller reorientation under an external magnetic field. The successful preparation of Fe_3O_4 magnetic nanoplatelets together with exfoliated and highly ordered zein resin nanocomposites was confirmed by scanning electron microscopy, X-ray diffraction, and a vibrating sample magnetometer. As a result, in comparison to zein resin film, the exfoliated zein nanocomposites (Fe-Zein) showed dramatic improvement on mechanical and barrier properties. The tensile strength, elongation, and Young's modulus of Fe-Zein were increased by 218, 48, and 264%, respectively, while the water vapor and oxygen permeability decreased by 68 and 29%. More importantly, the highly ordered zein nanocomposites (Fe-Zein-Mag) showed additional improvement on the mechanical and gas barrier properties. In comparison to Fe-Zein, the tensile strength and elongation of Fe-Zein-Mag were increased by 10 and 48%, respectively, and a 30% decrease in Young's Modulus was observed, indicating the Fe-Zein-Mag film was more elastic. Besides, the water vapor and oxygen permeability of Fe-Zein-Mag were also decreased by an additional 48 and 17%, respectively.

KEYWORDS: *Nanocomposite, highly ordered structure, biopolymer, mechanical property, gas barrier property*

INTRODUCTION

Over the past few decades, because of the functionality, lightweight, inexpensiveness, and ease of processing of polymers, they have replaced conventional metal or ceramic materials in ubiquitous packaging areas, where they provide physical, chemical, and biological protection from the environment and prolong product display. However, along with the arisen concern of environmental sustainability, the global sustainable packaging industry is growing much faster than the traditional packaging industry.[1] Biopolymers are considered as potential replacements for these conventional plastic packaging materials because of their superior biodegradability in nature. Although previous studies have shown their enormous versatility,[2−7] a limiting property of biopolymers used as packaging materials is their intrinsic mechanical property and barrier property to gaseous substances, such as water vapor, oxygen (O_2), carbon dioxide (CO_2), and organic volatile molecules.[4,6] The physical nature of these biopolymer materials resulted in great interests in developing new materials with enhanced vapor and/or gas barrier property by new preparation strategies and carrying out fundamental research to assist the understanding of the relationship between the polymer structure and its properties.

The most frequently adopted strategies to improve mechanical and gas barrier properties are the use of polymer composites, the coating of high-barrier materials, and the use of multilayered films consisting of a layer of high-barrier film.[8] Polymer composite is the most frequently adopted method, which is to add suitable filler into the polymer matrix to enhance the properties of polymer. Composites typically consist of a polymer matrix as the continuous phase and fillers as the discontinuous phase.[7−11] Nanocomposites are an innovative alternative to traditional technologies for improving polymer properties using nanoscale materials as fillers. Nanocomposites usually exhibit increased mechanical strength, improved gas/vapor barrier properties, and improved heat resistance compared to conventional polymers and polymer composites.[8,10,12] When dispersed into the polymer matrix, nanofillers create a maze-like structure that creates a tortuous path to gaseous molecules, greatly slowing their permeation rates.[9] Besides, traditional composite structures usually require large quantities of filler (~60 vol %), but the demand of nanofillers has been dramatically reduced in nanocomposites to <2 vol %.[10]

Plenty of studies have endeavored in the development of nanocomposite materials.[6,8,10,12,13] Currently, three types of polymer nanofiller structures have been well-achieved and studied: (a) tactoid, (b) intercalated, and (c) exfoliated[8,14] (Figure 1). Tactoid structures can be found in traditional composites.[13] Intercalated structures have moderate expansion of the clay interlayer, in which polymer chains can penetrate the basal spacing of the filler but the stacked shape of the nanoplatelets remains. In exfoliated structures, clay clusters lose their layered structure and are well-dispersed as individual nanoplatelets within the continuous polymer phase.[8,10] The current "ideal" structures for biopolymer nanocomposites are intercalated and exfoliated structures.[7−10,13] However, Bhar-

Received: February 8, 2012
Revised: April 3, 2012
Accepted: April 4, 2012
Published: April 4, 2012

dx.doi.org/10.1021/jf3005417 | J. Agric. Food Chem. 2012, 60, 4162−4169

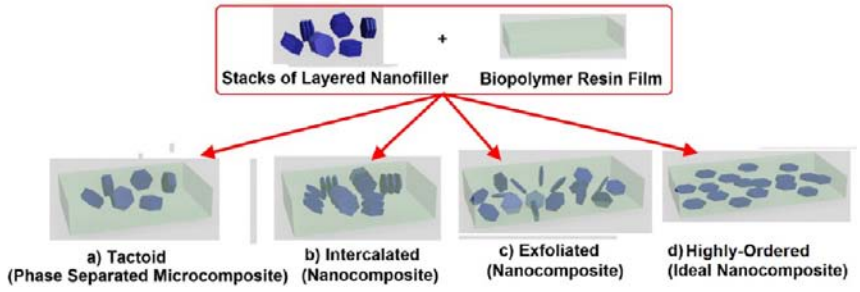

Figure 1. Four types of nanocomposite structures.[8]

adwaj has theoretically proven that highly ordered nanofillers (shown in Figure 1d, picture of highly ordered) could substantially increase the gas barrier properties by up to 3-fold compared to the intercalated or exfoliated structure following eq 1[9]

$$\frac{P_s}{P_p} = \frac{1 - \Phi_s}{1 + \frac{L}{2W}\Phi_s\left(\frac{2}{3}\right)\left(S + \frac{1}{2}\right)} \quad (1)$$

$$S = \frac{1}{2}(3\cos^2\theta - 1) \quad (2)$$

where L and W are the length and width of the nanofiller, respectively. S stands for the arrangement of the nanofiller (eq 2) and can be calculated by substituting the difference in angular value (θ) in eq 2. In a complete disordered filler arrangement, S is assigned as 0. In an ideal orthogonal arrangement, θ is 90°; therefore, S equals $-1/2$. In an ideal planar arrangement, where nanofillers are incorporated parallel to the nanocomposite interface, θ is 0° and S equals 1. Although the exfoliated structure consisted of well-distributed nanofillers in biopolymer matrices, the randomly orientated nanofillers cannot provide the optimized functionalities, including mechanical properties, gas permeability, electronic and catalytic properties, etc. Therefore, a highly ordered structure should be characterized as the nanofillers that are incorporated in polymer matrices in the way of both sufficient distribution and identical orientation. Recently, plenty of studies have pointed out the significance of synthesizing truly highly ordered nanocomposites.[6−10,12,13] More importantly, highly ordered nanocomposites have shown promising capabilities of improving the mechanical property and gas permeability of the matrix film, which were two critical characteristics to biopolymer-based packaging materials.[9,15,16]

Currently, several methods have been established in the formation of highly ordered nanocomposites, including dip-pen nanolithography[17] and layer-by-layer deposition.[18] Gao et al. established a pulse laser deposition method that incorporated layers of $CoFe_2O_4$ nanoarray in continuous $Pb(Zn, Ti)O_3$ alloys, and the as-prepared nanocomposite exhibited strong piezoelectric signals and magnetoelectric coupling.[17] Tian and his colleagues developed a method adopting electrostatic interaction.[18,19] The highly ordered structure was obtained by layer-by-layer deposition of positively charged poly(ethylamine) and a single-wall carbon nanotube functionalized with negatively charged sodium dodecylbenzenesulfonate. Although these two methods could form highly ordered structures of nanocomposite coating, their feasibility in sustainable packaging application is questionable because of the complexity of the fabrication techniques and impracticability in the scaled-up production of free-standing films. Therefore, to establish a low-cost and fast production of highly ordered biopolymer nanocomposites, a hydrothermal synthetic route to hexagonal magnetic nanoplatelets has been developed in this study, and the formed nanofillers have been characterized as well. Moreover, the highly ordered nanofillers through *in situ* reorientation have been produced by an external magnet. The mechanical and gas barrier properties of the zein film with or without adding nanofillers have been examined.

Zein was selected as the model biopolymer for its potential application as a structural packaging material.[20−22] Zein is a storage protein in corn kernel and is a major co-product from the biofuel industry. Its film-forming property has been recognized for decades.[20,23−25] However, the poor mechanical and gas barrier properties fundamentally restricted the application of zein and many other biopolymers as well. Scientists have endeavored in developing various methods to improve the properties of zein film, including plasticizer (e.g., polyols, mono-, di-, or oligosaccharides, lipids, and lipid derivatives),[20−23,25] coating of the moisture barrier (e.g., tung oil and linseed oil), as well as lamination.[26,27] Recent studies investigated a nanocomposite method that dramatically improved the properties of zein resin film using silica-based nanofillers.[28] However, it is still largely unachieved to form highly ordered nanocomposites, which would maximize the effects of nanofiller incorporation. Therefore, the objective of this study, is to develop a simple and cost-effective method to synthesize highly ordered biopolymer nanocomposites to improve tensile and gas barrier properties, using magnetic nanofillers, and zein is selected as the model biopolymer matrix.

MATERIALS AND METHODS

Materials. Zein was obtained from MP Biomedicals (Solon, OH), with a minimum of 90% protein. Oleic acid ($C_{18:1}$) was purchased from Fisher Scientific (Fairlawn, NJ). Hydrazine monohydrate ($N_2H_4{\cdot}H_2O$), ferrous sulfate, 7-hydrage ($FeSO_4{\cdot}7H_2O$), sodium hydroxide (NaOH), calcium sulfate anhydrous ($CaSO_4$), and magnesium nitrate [$Mg(NO_3)_2$] were purchased from Alfa Aesar (Ward Hill, MA).

Preparation of Iron(II, III) Oxide/Magnetite (Fe_3O_4) Nanoplatelet Filler. Hexagonal Fe_3O_4 nanoplatelet was prepared following Wang's method, with some modification.[29] N_2 degassed water was used for the preparation of 0.1 M $FeSO_4{\cdot}7H_2O$ aqueous solution. A total of 15 mL of Fe^{2+} solution was added to a Teflon-lined stainless autoclave (acid digestion bomb 4749, Parr Instrument Company, Moline, IL). A total of 5 mL of sufficiently mixed $N_2H_4{\cdot}H_2O$ aqueous solution (50%, v/v) with 0.6 g of NaOH was drop-wisely added to the Teflon linear under vigorous stirring. N_2 was continuously passed through the solvent to prevent Fe^{2+} oxidation. The autoclave was then placed in an oven at 130 °C for 6 h for reaction. After cooling to room temperature, the products were washed 3 times with water and ethanol and finally dried by a nitrogen evaporator (N-EVAP 111, Organomation Associates, Inc., Berlin, MA) at 25 °C for 3 h.

Preparation of the Fe_3O_4-Loaded Zein Resin Film. Zein resin was first prepared by dissolving granular zein in 70% ethanol aqueous solution (16%, w/v). Oleic acid was weighed separately at a ratio of 1 g/g of zein and homogenized at 10 000 rpm for 2 min with 2% by weight of as-prepared Fe_3O_4 nanofiller to ensure that the filler is well-distributed and protected by oleic acid using a homogenizer (VDI 25, VWR, West Chester, PA). The mixture was then added slowly into heated zein solution at 75 °C and stirred vigorously for 15 min. Thereafter, the above emulsion was poured into an ice water bath (0 °C) to obtain the zein-based resin. After kneading, zein films were prepared by stretching the dough over the circular rims of the Petri dish. Films were air-dried for 24 h under room conditions. After drying, film stacks of 3 ply were laminated (fusion type) at 120 °C for 5 min under a commercial hot roller (Apache AL-13P) to produce the final specimen with an exfoliated filler structure (Fe-Zein) for further characterization. Besides, zein−oliec acid resin films without the addition of Fe_3O_4 nanofiller were prepared as the control, which was denoted as "Zein".

Formation of the Highly Ordered Fe_3O_4 Nanofiller in Zein Resin. The highly ordered Fe_3O_4 nanofiller in zein resin should be both well-distributed and highly aligned. To obtain this structure, the as-prepared exfoliated Fe-Zein films were further treated with a 4 kG external magnetic field under a permanent magnet (Neodymium Magnets N52, Protage, IN) over a hot plate at 120 °C for 20 min. The final highly ordered films (Fe-Zein-Mag) were then cooled to room temperature before the removal of the magnet.

Scanning Electron Microscopy (SEM). The morphology and orientation of nanofillers were examined by SEM (SU-70, Hitachi, Pleasanton, CA). First, the Fe_3O_4 nanofiller and resin film samples were mounted on a specimen stub by conductive carbon tape, and then the stub was coated with a layer of conductive gold particle (~20 nm) with a sputter coater (Hummer XP, Anatech, CA). Representative SEM images were then depicted and analyzed in the following section.

X-ray Diffraction (XRD). XRD was used to characterize the chemical composition of the nanofiller and the nanofiller orientation inside zein resin films. Nanofiller powder and resin films were attached to specimen stubs by flat double-sided tape. Powder diffraction was measured using a Bruker D8 Advance powder diffractometer operated in Bragg−Brentano mode (θ–θ geometry), equipped with a Cu$K\alpha$ sealed tube (wavelength of 1.541 78 Å), Ni β-filter, and position-sensitive LynxEye detector. After measurement, phase identification was performed using the International Center for Diffraction Data (ICDD) powder diffraction database.

Vibrating Sample Magnetometer (VSM). The magnetic property of the as-prepared Fe_3O_4 nanofiller and nanocomposite film was investigated by VSM (Lakeshore 7400, Westerville, OH). The powdered Fe_3O_4 nanofiller (10 mg) was filled inside a Kel-F sample holder cup, while nanocomposites films (10 × 10 × 0.76 mm) were attached to a Kel-F thin-film bottom sample tail during the measurement. The field intensity was scanned from 5 to −5 kG. The homogeneity and anisotropy of the nanofillers were determined by combining in-plane (IP) and out-of-plane (OOP) hysteresis loops. All experiments were performed at 20 °C.

Tensile Property. The tensile property, including tensile strength, elongation, and Young's modulus, was measured using a texture analyzer (TA.XT plus, Stable Micro System, Surrey, U.K.). The tensile tests were performed according to American Society for Testing and Materials (ASTM) Standard Method D638-10.[26,27] Film thickness was measured with a graduation micrometer (General Tools, New York City, NY). Zein film specimens were first cut into dumbbell shape of type I dimension and then were preconditioned at 23 °C and 53% relative humidity (RH) [saturated $Mg(NO_3)_2$] for 48 h. The texture analyzer was set to an initial grip of 115 mm and an extension rate of 5 mm/min. Five replicates were measured for each treatment.

Water-Vapor Permeability. The water-vapor permeability of zein resin films was measured gravimetrically, according to ASTM Standard Method E96/E96M-10.[26,27] Test cells had an exposure area of 10 cm^2 (PO-2300, BYK, Columbia, MD). $CaSO_4$ anhydrous was used to maintain 0% RH inside the cells. Saturated solutions of $Mg(NO_3)_2$ and deionized water were placed in sorbostats to maintain 53 and 100% RH at 25 °C, respectively. Weight gains were plotted versus time, and a steady state was assumed as a straight line fitting six points of the plot. Three replicates were measured for each treatment.

Oxygen Gas Permeability. The O_2 permeability was measured using a non-invasive oxygen analysis system (Oxy-Sense 101, Dallas, TX) according to ASTM Standard Methods F2714-08 and F2622-08e1.[26,27] The stainless-steel test cell had an exposure area of 10 cm^2, and the OXYDOT oxygen sensor (Oxysense, Dallas, TX) was attached to the window at the bottom of the test cell. After carefully sealing the test cell to avoid film wrinkle, pure nitrogen gas was prefilled at the bottom chamber of the test cell prior to the experiment. Then, the test cell was stored at 20 °C and 36% humidity in dark until the equilibrium condition was established.

Statistical Analysis. The data of tensile and gas barrier properties were reported as the mean ± standard error, and the experimental statistics were performed using the SAS software with $\alpha = 0.05$ (version 9.2, SAS Institute, Inc., Cary, NC).

RESULTS AND DISCUSSION

Synthesis of Magnetic Nanoplatelet Nanofillers. In this study, Fe_3O_4 hexagonal nanoplatelets were synthesized by the hydrothermal method and the representative SEM image was shown in Figure 2a. The nanofiller should be specifically prepared to achieve both a high aspect ratio and magnetic property. According to the theoretical model by Bharadwaj, the high aspect ratio (e.g., nanoplatelet) is critical to provide better gas barrier and mechanical support.[9] As characterized by SEM, the nanofillers showed the shape of a hexagonal plate, which had a high aspect ratio, and the size of an individual platelet was around 200 × 20 nm (long diagonal × height). Besides, the chemical composition and magnetic property of the nanofiller were determined using XRD and VSM, and results were presented in panels b and c of Figure 2, respectively. The XRD spectrum showed a perfect match over a standard Fe_3O_4 spectrum in the ICDD database. The strongest signal peak of plane (311) reflection would be used to identify the presence of the Fe_3O_4 nanofiller in the following characterization of nanocomposites. The magnetic property of the filler was also confirmed by the VSM. The thin loop indicated that the Fe_3O_4 nanoplatelet had a small coercive force and soft ferromagnetic property (Figure 2c). Similar results have been reported for the other Fe_3O_4-based nanomaterials in various shapes.[30]

Formation of Exfoliated Nanocomposites. In previous studies, it was found that only intercalated and exfoliated nanocomposites could significantly improve the mechanical and gas barrier properties of packaging materials because of the sufficient distribution of nanofillers in the packaging matrix. The tactoid structures were found to be a physical blend of two components because of the poor compatibility between filler and matrix materials.[8,10,13,14] The shearing forces with high energy (i.e., homogenization process) were applied in this study to enable the sufficient separation of nanoplatelets, among which the primary interplanar interaction was strong magnetic forces rather than weak hydrogen bond and hydrophobic−hydrophobic attraction. Dispersion of nanoplatelets into the polymer matrix is affected by mismatches between the hydrophobic−hydrophilic character of both the filler and biopolymer matrices.[8,10] In this study, zein was hydrophobic[20] and nanofillers (Fe_3O_4) were hydrophilic. Therefore, to prepare the exfoliated nanocomposite (Fe-Zein), the surfaces of Fe_3O_4 nanofillers were modified with a surface-active component that was amphiphilic oleic acid molecules to improve the hydrophobicity and the compatibility with zein matrices. Consequently, an exfoliated nanocomposite was successfully

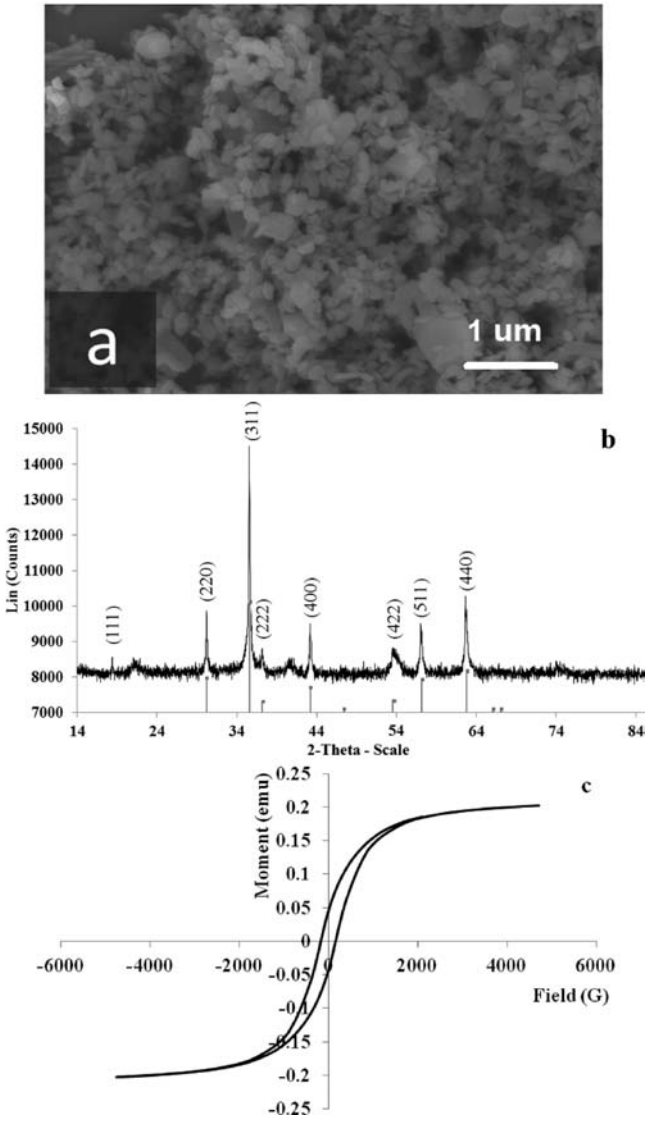

Figure 2. Characterization of the Fe_3O_4 nanofiller: (a) SEM image of the nanofiller showing its hexagonal nanocrystal shape, (b) XRD spectrum of the nanofiller and the peaks standard Fe_3O_4 in the ICDD database, and (c) hysteresis loop of the nanofiller determined by VSM.

obtained. The formed exfoliated structure was examined by SEM (Figure 3b), which showed that the magnetic nanofillers were well-distributed and incorporated into the flat zein resin film in a random orientation. Both perpendicular (dashed circle in Figure 3b) and parallel (solid circle in Figure 3b) orientation of nanofillers to the planar surface were found in the resin film. The XRD spectrum further confirmed the successful incorporation of Fe_3O_4 nanofillers by showing a typical plane (311) reflection of a Fe_3O_4 crystal compared to the control of the zein resin film (Figure 4). Besides, the proposed incorporation of the magnetic nanofiller in the polymer film has also been confirmed by the VSM result (Figure 5). The hysteresis loops of the IP and OOP scan of the exfoliated nanocomposites showed similar shape. Besides, Fe-Zein-IP and Fe-Zein-OOP showed similar residue flux density values (y-axis intercept) around 0.0005 emu. These results indicated that the magnetic nanofillers in exfoliated nanocomposites were well-distributed and randomly orientated. According to the Stoner–Wohlfarth model, an anisotropic material should behave differently in response to various directions of external magnetic fields.[31] Because the IP and OOP loops in the Fe-Zein sample overlapped with each other, the magnetic nanofillers in Fe-Zein were randomly oriented, indicating that a typical exfoliated structure was formed. Therefore, the results of the SEM image, XRD spectrum, and VSM hysteresis loops proved the successful formation of exfoliated Fe-Zein nanocomposites filled with well-distributed and randomly oriented Fe_3O_4 nanoplatelets.

Formation of Highly Ordered Nanocomposites. The highly ordered nanocomposite (Fe-Zein-Mag) was obtained from the heat- and magnetic-treated exfoliated nanocomposite (Fe-Zein). The nanofillers in Fe-Zein-Mag should have property of both exfoliated structure and highly aligned in orientation. As shown in Figure 6, fillers were mostly embedded in one direction, parallel to the resin film (solid circle in the figure), which was very similar to the schematic top view of the highly ordered nanocomposite (Figure 1, picture of highly ordered). The typical peak of the Fe_3O_4 crystal in the XRD spectrum was identified from the zein resin background (Figure 7a) for the Fe-Zein-Mag sample. Besides, a close comparison of the signal of plane (311) reflection between Fe-Zein and Fe-Zein-Mag further provided supporting information (Figure 7b) to filler orientation. The peak shown in the Fe-Zein-Mag spectrum was narrower and sharper than the peak in the Fe-Zein spectrum, which indicated that the Fe_3O_4 filler was more uniformly oriented in the Fe-Zein-Mag sample and some anisotropic structures may present.[32] The magnetic property of Fe-Zein-Mg (Figure 8) obtained from VSM was different from that of Fe-Zein (Figure 5). An increase of the residue flux density was observed in Fe-Zein-Mag-OOP to over 0.000 65 emu from 0.0005 emu in Fe-Zein-OOP, while the value in Fe-Zein-Mag-IP decreased to 0.0004 emu. It was reported that the magnetic dipole of the nanoplatelet was perpendicular to the Fe_3O_4 nanocrystal plane,[33] so that the increase in the OOP direction and the decrease in the IP direction indicated that a

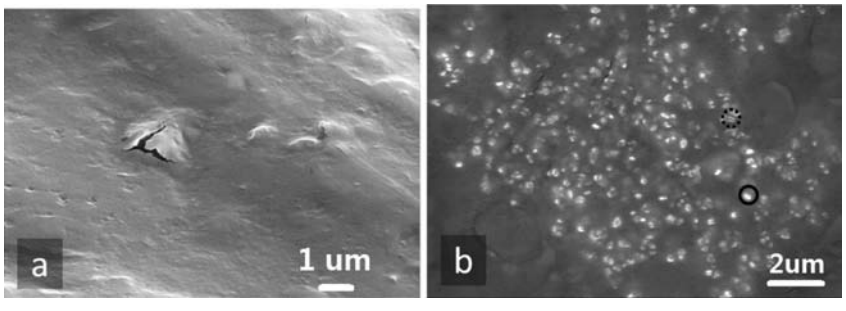

Figure 3. SEM image of (a) zein resin film (Zein) and (b) exfoliated nanocomposite (Fe-Zein).

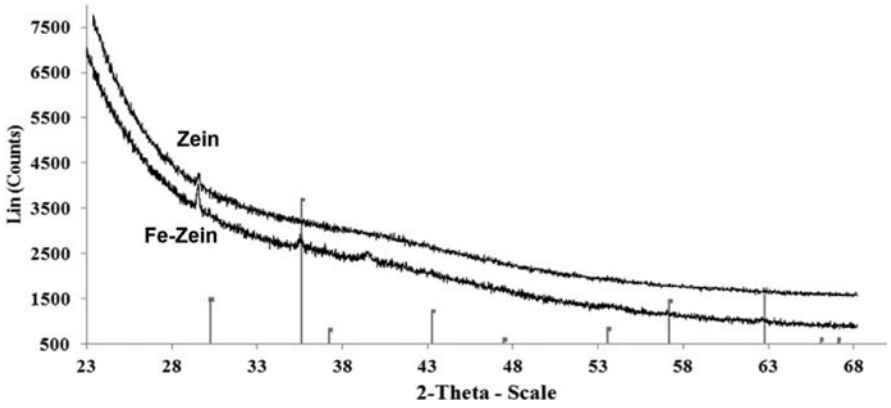

Figure 4. XRD spectra of zein resin film (Zein) and exfoliated nanocomposites (Fe-Zein).

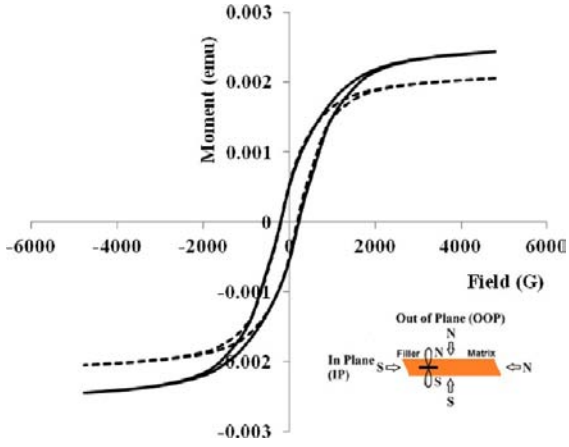

Figure 5. Hysteresis loops of exfoliated nanocomposites (Fe-Zein) in IP (solid loop) and OOP (dashed loop) directions.

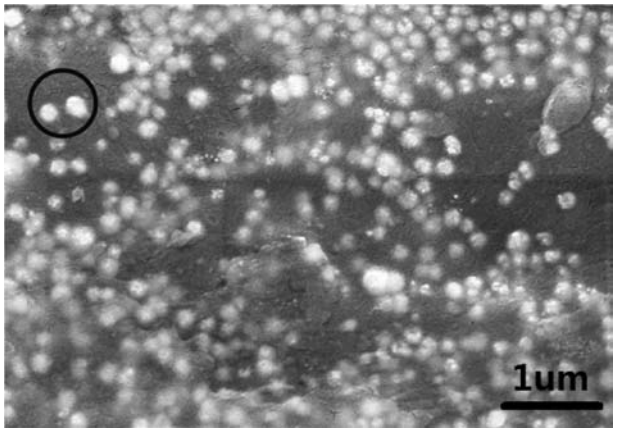

Figure 6. SEM image of highly ordered nanocomposites (Fe-Zein-Mag).

majority of nanofillers was parallel to the film, with their magnetic dipoles perpendicular to the film plane, which was in agreement with SEM results. The relationship between nanomagnetite orientation and the magnetic property was also confirmed by previous studies that the shapes of OOP and IP loops were significantly different in an anisotropic material.[31] All together, the SEM, XRD, and VSM results confirmed the effects of the external magnetic field on the structure inside nanocomposites. The rearrangement of highly ordered nanofillers was achieved by applying an *in situ* external magnet.

Tensile Property. The tensile properties, including tensile strength, elongation, and Young's modulus, were measured for treatments of zein films (Zein), zein films with exfoliated nanocomposites (Fe-Zein), and highly ordered nanocomposites (Fe-Zein-Mag), and results were reported in Table 1. The zein resin film was selected as a control. However, the mechanical property of the control zein film obtained in this study was lower than those of the previously reported zein resin film.[26,27] This can be attributed to the different conditions in the lamination process that low-pressure lamination was adopted in this study, while high-pressure carver press was used in previous studies.[26,27] Nonetheless, after adding the nanofiller, the exfoliated nanocomposite Fe-Zein showed a dramatic improvement in both tensile strength (by 218.0%), Young's modulus (by 264.6%), and elongation (by 48.3%) compared to the blank zein resin film, which could be attributed primarily to the change of film composition and the formation of the exfoliated structure. A similar phenomenon has been discovered by various studies using silica-based nanofillers[28] that the 2% loading of the montmorillonite nanofiller in the exfoliated nanocomposite showed approximately 140 and 150% increase in tensile strength and Young's modulus, respectively. After nanofiller reorientation, the Fe-Zein-Mag sample showed more elastic behavior indicated by the decreased Young's modulus (from 344 to 240 MPa), while the elongation further increased by another 47.7%. Moreover, the tensile strength of treated films showed an increase but was not significantly different from that of the control zein film. During the tensile testing, the external force was parallel to the resin film and in the same direction as the orientation of the nanofiller in Fe-Zein-Mag, in which the fillers "anchored" among different polymer molecules and provided a strengthened intermolecular attraction against deformation. We thought that the synthesized hexagonal Fe_3O_4 nanoplatelet had a similar function as the role of the silica nanoplatelet in improving the mechanical property of the biopolymer film, while providing additional magnetic property to manipulate fillers *in situ* at nanoscale.

Barrier Property. *Water Vapor Permeability.* The moisture and gas barrier property is another critical feature in determining the applicability of a biopolymer film as a packaging material. Similar to the mechanical properties, the water vapor permeability of zein resin film obtained in this study was also higher than the reported value[26,27] because of the involvement of the low-pressure lamination process. However, after the nanocomposites were formed, the water

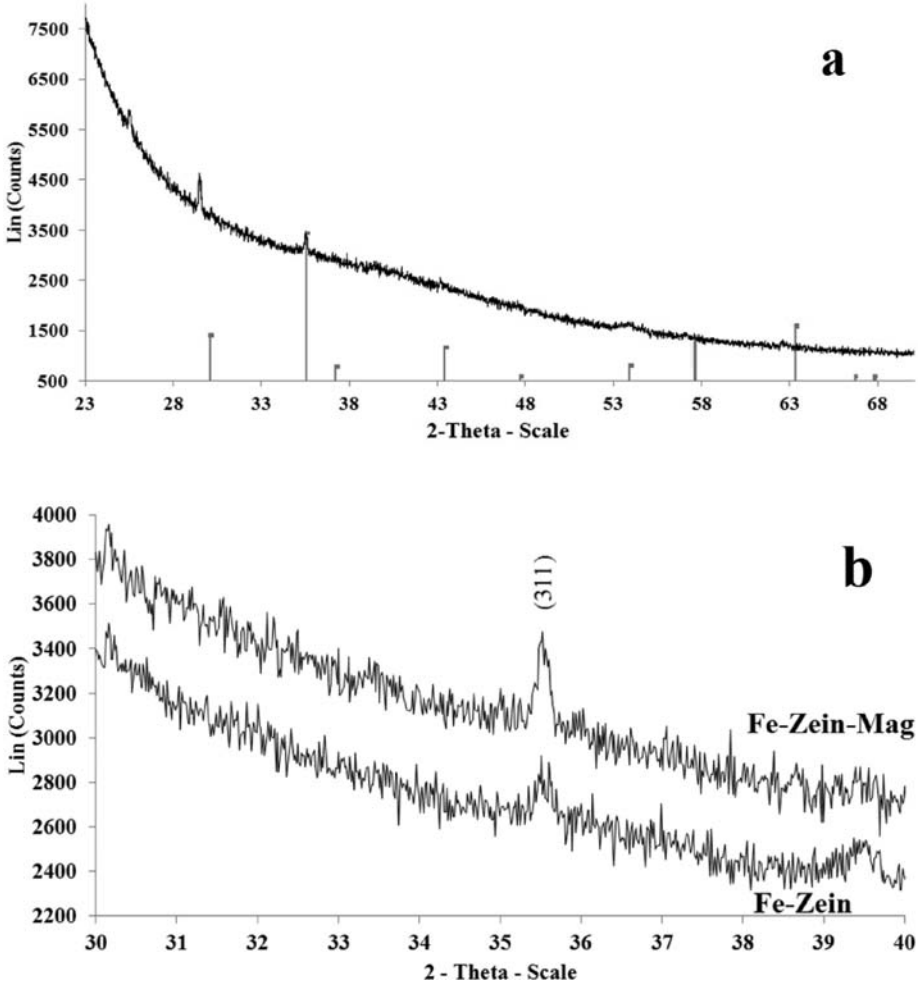

Figure 7. XRD spectra of (a) highly ordered nanocomposites (Fe-Zein-Mag) and (b) comparison of plane (311) reflection of the Fe_3O_4 nanofiller in exfoliated nanocomposites (Fe-Zein) and highly ordered nanocomposites (Fe-Zein-Mag).

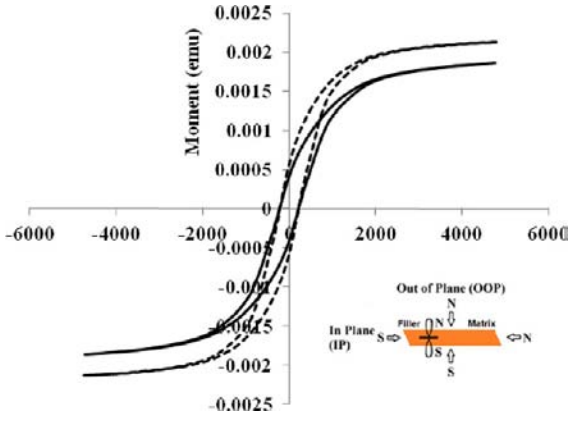

Figure 8. Hysteresis loops of the highly ordered nanocomposite (Fe-Zein-Mag) in IP (solid loop) and OOP (dashed loop) directions.

vapor permeability of the exfoliated Fe-Zein sample was decreased 32 and 45% compared to that of the control zein resin film at 53 and 100% RH, respectively. A previous study[28] using 2% loading of layered silica in zein film also achieved similar effects that the water vapor permeability decreased by 38% at 52% RH. Therefore, the result indicated that the Fe_3O_4 nanofillers had a similar function as the layered silica, commonly used filler. In agreement with the theoretical modeling[9] and other previous research studies,[28] the inorganic nanofillers (e.g., Fe_3O_4 or silica) were impermeable to water and gaseous molecules, because of the close packing substructure in their nanocrystal platelets. On the basis of the theoretical model by Bharadwaj,[9] as shown in eq 2, the vapor permeability of nanocomposites with highly ordered arrangement ($S = 1$) could be as low as one-third of that of exfoliated nanocomposites ($S = 0$). In this study, the highly ordered nanocomposites only showed an additional 48 and 34% drop of

Table 1. Thickness and Tensile Properties of Zein-Based Nanocomposites[a]

sample name	thickness (10^{-4} m)	tensile strength (MPa)	elongation at break (%)	Young's modulus (MPa)
Zein	7.95 ± 1.17 b	2.11 ± 0.35 b	24.05 ± 4.73 c	94.50 ± 35.79 c
Fe-Zein	5.69 ± 0.33 c	6.71 ± 0.95 a	35.67 ± 1.67 b	344.57 ± 14.76 a
Fe-Zein-Mag	12.78 ± 0.84 a	7.39 ± 0.36 a	52.67 ± 7.67 a	239.78 ± 10.24 b

[a]Means with the same letter are not significantly different ($p > 0.05$).

dx.doi.org/10.1021/jf3005417 | J. Agric. Food Chem. 2012, 60, 4162–4169

the permeation rate at 53 and 100% RH, respectively. The difference between the experimental results and the theoretical anticipation could be ascribed to the nonhomogeneous distribution of the nanofillers inside the resin film (Figure 3b), even though most of them faced the same direction. Besides, it can be seen in Table 2 that the water vapor permeability in 100% RH was much higher than that in the 53% environment, and the effects of the incorporation and orientation of fillers were also diminished in the high-moisture circumstance. Similar phenomena were previously reported by Lai et al.,[22] in which they associated the phenomena with the swelling of the zein resin film in a high-moisture environment. The swelling and the moisture adsorption inside the resin film may impair the integrity of the film and result in defects on the formation of the moisture channel for water migration.

Table 2. Gas Barrier Properties of Zein-Based Nanocomposites[a]

sample name	water vapor permeability 53% RH (pg Pa^{-1} s^{-1} m^{-1})	water vapor permeability 100% RH (pg Pa^{-1} s^{-1} m^{-1})	O_2 permeability (10^{-18}, m^2 Pa^{-1} s^{-1})
Zein	58.51 ± 13.22 a	69.26 ± 17.99 a	685.1 ± 52.8 a
Fe-Zein	18.91 ± 3.66 b	31.58 ± 6.12 b	488.3 ± 44.6 b
Fe-Zein-Mag	9.83 ± 4.29 c	20.95 ± 4.15 c	403.9 ± 39.4 c

[a]Means with the same letter are not significantly different ($p > 0.05$).

O_2 Permeability. Oxygen permeability is another useful characteristic in the application of the biopolymer film. Similar to the result of water vapor permeability, Fe_3O_4 nanofillers provided a barrier to oxygen gas. After loading 2% nanofillers in zein resin film, the O_2 permeability of Fe-Zein dropped 28.7% from that of the zein control film. Besides, the highly ordered nancomposite (Fe-Zein-Mag) showed further improvement by 17.3% to provide a better physical barrier to O_2. The improvement in O_2 barrier property was only half of that in water vapor. An earlier study ascribed this effect to the incorporation of plasticizer oleic acid.[26,34] They found that oleic acid can absorb free gaseous oxygen to the resin film and facilitate the permeation of the oxygen molecule through the film. Because oleic acid was added to the zein film at the ratio of 1:1 (w/w), it may have contributed to the O_2 permeability and counterbalance of the contribution of 2% loaded Fe_3O_4 nanofillers.

In summary, Fe_3O_4 magnetic nanoplatelets with a high aspect ratio were successfully synthesized in this study using a simple hydrothermal reaction. The prepared nanoplatelet was used as nanofillers to form zein nanocomposites and improve mechanical and gas barrier properties of zein films (Scheme 1). The structure and chemical composition of both random-oriented (exfoliated) and highly ordered were confirmed by SEM, XRD, and VSM. Further investigation revealed that highly ordered nanofillers can further improve the elasticity and gas barrier properties of zein films, which was predicted by the theoretical study by Bharadwaj. Therefore, this study successfully confirmed the feasibility of preparing highly ordered nanocomposites using high aspect ratio magnetic nanofillers. Besides, this method was simpler and more cost-effective compared to the aforementioned lithography and layer-by-layer deposition methods and may bring an impact on further improvement of the functionality and application of other biopolymer films. Nonetheless, to optimize the mechanical and gas barrier properties of biopolymer films, more work may be endeavored to resolve additional unknown questions, such as the potential environmental impact of the Fe_3O_4 nanofiller or reduce potential interference of iron oxide filler to the metal detector by developing other magnetic nanofillers using conventional nanofiller materials, such as a

Scheme 1. Scheme of (Top Left) Zein Resin Film, (Bottom Left) Fe-Zein Exfoliated Nanocomposite Film, and (Bottom Right) Fe-Zein-Mag Highly Ordered Nanocomposite Film[a]

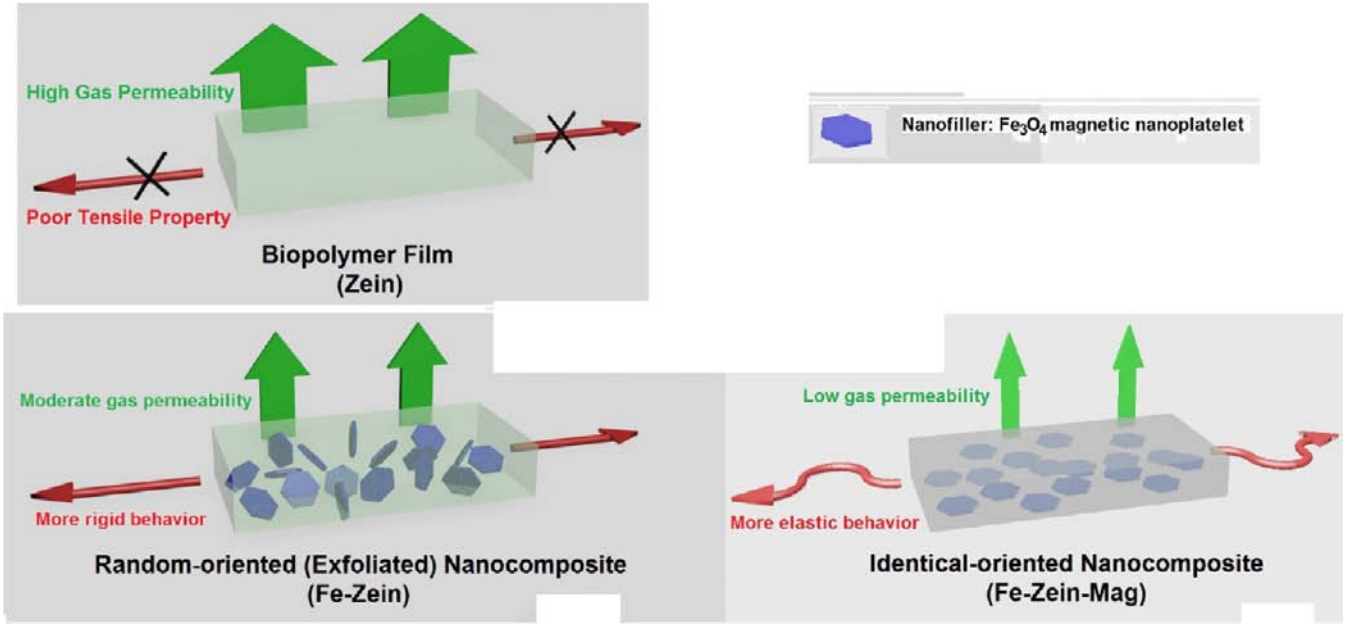

[a]The size of the red arrow indicated the level of the gas permeability rate (VP, vapor pressure; RH, relative humidity). The shape of the blue arrow indicated the prominent tensile property of the film (straight arrow, rigid property; curved arrow, elastic property).

graphene sheet or layered silica doped with a trace amount of iron ions.

AUTHOR INFORMATION

Corresponding Author

*Telephone: (301) 405-8421. Fax: (301) 314-3313. E-mail: wangqin@umd.edu.

Funding

We acknowledge the support of the Maryland NanoCenter at the University of Maryland.

Notes

The authors declare no competing financial interest.

ACKNOWLEDGMENTS

Appreciation goes to Dr. Peter Zavalij for his kind interpretation on XRD results and Dr. Ichiro Takeuchi and Dr. Tieren Gao for their professional assistance on VSM experiments. We specially thank Dr. Yaguang Luo and Dr. Robert Saftner for allowing us to use the O_2 permeability facility.

REFERENCES

(1) Platt, D. *Biodegradable Polymer—Market Report*; Smithers Rapra Limited: Shropshire, U.K., 2006.

(2) Marsh, K.; Bugusu, B. Food packaging—Roles, materials, and environmental issues. *J. Food Sci.* **2007**, *72*, R39–R55.

(3) Mukherjee, T.; Kao, N. PLA based biopolymer reinforced with natural fibre: A review. *J. Polym. Environ.* **2011**, *19*, 714–725.

(4) Kumar, P.; Sandeep, K. P.; Alavi, S.; Truong, V. D. A review of experimental and modeling techniques to determine properties of biopolymer-based nanocomposites. *J. Food Sci.* **2011**, *76*, E2–E14.

(5) Kriegel, C.; Arrechi, A.; Kit, K.; McClements, D. J.; Weiss, J. Fabrication, functionalization, and application of electrospun biopolymer nanofibers. *Crit. Rev. Food Sci.* **2008**, *48*, 775–797.

(6) Rhim, J. W. Potential use of biopolymer-based nanocomposite films in food packaging applications. *Food Sci. Biotechnol.* **2007**, *16*, 691–709.

(7) de Azeredo, H. M. C. Nanocomposites for food packaging applications. *Food Res. Int.* **2009**, *42*, 1240–1253.

(8) Ray, S. S.; Okamoto, M. Polymer/layered silicate nanocomposites: A review from preparation to processing. *Prog. Polym. Sci.* **2003**, *28*, 1539–1641.

(9) Bharadwaj, R. K. Modeling the barrier properties of polymer-layered silicate nanocomposites. *Macromolecules* **2001**, *34*, 9189–9192.

(10) Ray, S. S.; Bousmina, M. Biodegradable polymers and their layered silicate nano composites: In greening the 21st century materials world. *Prog. Mater. Sci.* **2005**, *50*, 962–1079.

(11) Zhang, B.; Luo, Y.; Wang, Q. Development of silver/α-lactalbumin nanocomposites: A new approach to reduce silver toxicity. *Int. J. Antimicrob. Agents* **2011**, *38*, 502–509.

(12) Sorrentino, A.; Gorrasi, G.; Vittoria, V. Potential perspectives of bio-nanocomposites for food packaging applications. *Trends Food Sci. Technol.* **2007**, *18*, 84–95.

(13) Alexandre, M.; Dubois, P. Polymer-layered silicate nanocomposites: Preparation, properties and uses of a new class of materials. *Mater. Sci. Eng., R* **2000**, *28*, 1–63.

(14) Carrado, K. A. Synthetic organo- and polymer-clays: Preparation, characterization, and materials applications. *Appl. Clay Sci.* **2000**, *17*, 1–23.

(15) Salvetat, J. P.; Kulik, A. J.; Bonard, J. M.; Briggs, G. A. D.; Stockli, T.; Metenier, K.; Bonnamy, S.; Beguin, F.; Burnham, N. A.; Forro, L. Elastic modulus of ordered and disordered multiwalled carbon nanotubes. *Adv. Mater.* **1999**, *11*, 161–165.

(16) Wong, E. W.; Sheehan, P. E.; Lieber, C. M. Nanobeam mechanics: Elasticity, strength, and toughness of nanorods and nanotubes. *Science* **1997**, *277*, 1971–1975.

(17) Gao, X. S.; Rodriguez, B. J.; Liu, L. F.; Birajdar, B.; Pantel, D.; Ziese, M.; Alexe, M.; Hesse, D. Microstructure and properties of well-ordered multiferroic $Pb(Zr,Ti)O_3/CoFe_2O_4$ nanocomposites. *ACS Nano* **2010**, *4*, 1099–1107.

(18) Tian, Y.; Park, J. G.; Cheng, Q. F.; Liang, Z. Y.; Zhang, C.; Wang, B. The fabrication of single-walled carbon nanotube/polyelectrolyte multilayer composites by layer-by-layer assembly and magnetic field assisted alignment. *Nanotechnology* **2009**, *20*, 7.

(19) Svagan, A.; Åkesson, A.; Cárdenas, M.; Bulut, S.; Knudsen, J.; Risbo, J.; Plackett, D. Transparent films based on PLA and montmorillonite with tunable oxygen barrier properties. *Biomacromolecules* **2012**, *13*, 397–405.

(20) Lai, H. M.; Padua, G. W. Properties and microstructure of plasticized zein films. *Cereal Chem.* **1997**, *74*, 771–775.

(21) Lai, H. M.; Padua, G. W.; Wei, L. S. Properties and microstructure of zein sheets plasticized with palmitic and stearic acids. *Cereal Chem.* **1997**, *74*, 83–90.

(22) Lai, H. M.; Padua, G. W. Water vapor barrier properties of zein films plasticized with oleic acid. *Cereal Chem.* **1998**, *75*, 194–199.

(23) Lawton, J. W. Zein: A history of processing and use. *Cereal Chem.* **2002**, *79*, 1–18.

(24) Zhang, B. C.; Luo, Y. C.; Wang, Q. Development of silver–zein composites as a promising antimicrobial agent. *Biomacromolecules* **2010**, *11*, 2366–2375.

(25) Zhang, B. C.; Luo, Y. C.; Wang, Q. Effect of acid and base treatments on structural, rheological, and antioxidant properties of α-zein. *Food Chem.* **2011**, *124*, 210–220.

(26) Rakotonirainy, A. M.; Padua, G. W. Effects of lamination and coating with drying oils on tensile and barrier properties of zein films. *J. Agri. Food Chem.* **2001**, *49*, 2860–2863.

(27) Wang, Q.; Padua, G. W. Properties of zein films coated with drying oils. *J. Agri. Food Chem.* **2005**, *53*, 3444–3448.

(28) Luecha, J.; Sozer, N.; Kokini, J. L. Synthesis and properties of corn zein/montmorillonite nanocomposite films. *J. Mater. Sci.* **2010**, *45*, 3529–3537.

(29) Wang, J.; Chen, Q. W.; Zeng, C.; Hou, B. Y. Magnetic-field-induced growth of single-crystalline Fe_3O_4 nanowires. *Adv. Mater.* **2004**, *16*, 137–140.

(30) Tan, Y.; Zhuang, Z.; Peng, Q.; Li, Y. Room-temperature soft magnetic iron oxide nanocrystals: Synthesis, characterization, and size-dependent magnetic properties. *Chem. Mater.* **2008**, *20*, 5029–5034.

(31) Wouters, J.; Lebedev, O. I.; Van Tendeloo, G.; Yamada, H.; Sato, N.; Vanacken, J.; Moshchalkov, V. V.; Verbiest, T.; Valev, V. K. Preparing polymer films doped with magnetic nanoparticles by spin-coating and melt-processing can induce an in-plane magnetic anisotropy. *J. Appl. Phys.* **2011**, *109*, No. 076105.

(32) Tomov, I. Accounting for secondary extinction in XRD characterizations of texture and microstructure with anisotropy—Responsive methods. *Arch. Metall. Mater.* **2005**, *50*, 147–157.

(33) Foss, S.; Proksch, R.; Dahlberg, E. D.; Moskowitz, B.; Walsh, B. Localized micromagnetic perturbation of domain walls in magnetite using a magnetic force microscope. *Appl. Phys. Lett.* **1996**, *69*, 3426–3428.

(34) Kanig, J. L.; Goodman, H. Evaluative procedures for film-forming materials used in pharmaceutical applications. *J. Pharm. Sci.* **1962**, *51*, 77–83.